

# Print Mask Design for Maximum Throughput Subject to Print Quality Constraints

J. William Boley and George T.-C. Chiu; Purdue University; West Lafayette, IN/USA

## Abstract

Many print-heads today consist of multiple nozzles. Hardware limitations and print quality requirements make it difficult to print from all nozzles or even adjacent nozzles at a given time. Print modes are established to trade-off between print speed and print quality requirements based on different media, ink, and image content. A print mask associates each pixel of the image with a pass number for a given print mode. Given a printing system, this study formulates a constrained optimization problem to generate all admissible print masks that maximize throughput (i.e. minimizes the number of passes) subject to constraints reflecting hardware limitations and print quality requirements. Two examples will be given to show the utility of these methods.

## Introduction

Many print-heads today consist of multiple nozzles. Figure 1 shows a schematic of a print-head array consisting of  $k$  nozzles. The column on the left is made up of odd numbered nozzles while the column on the right is comprised of even numbered nozzles. The columns are separated by a distance  $a$  in the print-head scan direction and the distance between nozzles in the media advance direction is  $b$ . As one can expect, arrays of multiple nozzles lead to higher throughput because they provide the ability to simultaneously deposit ink at multiple locations.

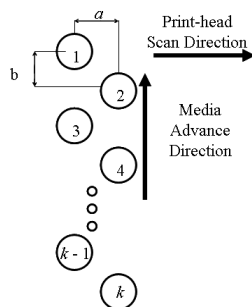


**Figure 1.** Schematic of an array of  $k$  nozzles with the Print-head Scan Direction and the Media Advance Direction defined.

In an ideal situation, we would have the print-head travel over the media in the print-head scan direction until reaching the width of the image, advance the length of the print-head ( $b \cdot k$ ) in the media advance direction, and repeat this process until reaching the end of the image (i.e. the print-head would visit each pixel of the image once and only once). However, hardware limitations and print quality requirements make it difficult to print from all nozzles or even adjacent nozzles at a given time. Print modes are established to trade-off between print speed and print quality requirements based on different media, ink, and image content. A multi-pass

print mode optimized for halftoned images may not be desirable or have adequate throughput for text or line art documents, which have higher requirements on swath alignment.

Since not all nozzles should be fired at any given pass for a multi-pass print mode, the print-head must pass over each pixel more than once so that there is more than one opportunity for ink deposition. Figure 2 shows how an image can be printed by two passes of a print-head with six nozzles.

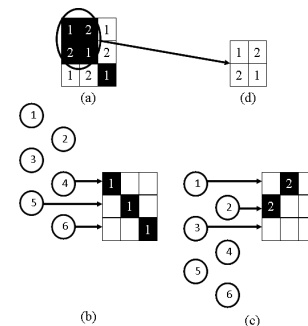


**Figure 2.** (a) Image to be printed, (b) Image printed during first pass, (c) Image printed during second pass, (d) Print mask used for printing image.

Figure 2(a) is the image to be printed. On the first pass, the bottom three nozzles pass over the image filling in the top left pixel with the fourth nozzle, the middle pixel with the fifth nozzle, and the bottom right pixel with the sixth nozzle (i.e. all of the pixels requiring ink which are labeled with pass number 1) as shown in Figure 2(b). The substrate then moves three nozzles in the media advance direction relative to the print-head. The print-head then passes over the image pixels its second and final time, printing the top middle pixel from the first nozzle and the middle left pixel from the second nozzle (i.e. all of the pixels requiring ink which are labeled with pass number 2) as illustrated in (Figure 2(c)). Figure 2(d) is the print mask (PM) used for printing the image, which is referred to in the literature [1,2] as the checkerboard design because of the checkerboard pattern of 1's and 2's in the PM. The checkerboard PM design is often used to avoid consecutive firing of the same nozzle and in some cases to avoid print artifacts like drop coalescence, among others. In some print applications, the checkerboard pattern may be adequate, but this is not the case in general. Due to print quality requirements and hardware limitations, PMs other than that of the checkerboard design may be needed.

Coalescence is one of the important factors that negatively affect print quality. The logic used in the literature [1,2] to avoid coalescence is to allow time for ink solvent to evaporate before depositing ink onto an adjacent pixel. However, no specific guidelines are given to determine the adequate time between drop depositions to avoid coalescence. Taking the checkerboard PM for

example, the time it takes to reach adjacent pixels on the second pass may be insufficient to allow for evaporation. In addition, diagonally adjacent pixels printed on the same pass may also coalesce. Recently a model has been developed to give a one-to-one correspondence from the probability of coalescence between two adjacent drops on a substrate to the time difference between their depositions [3]. Therefore, if an acceptable probability of coalescence is known a priori, then a minimum waiting time can be deduced.

Hardware limitations stemming from the geometry of the print-head must also be considered. To maintain nozzle orifice shape and avoid inter-nozzle drop formation interference, many nozzle arrays are manufactured with the staggered nozzle design shown in Figure 1. In addition the directionality associated with the nozzle array should also be considered when designing a *PM*. Droplet ejection frequency is another hardware limitation. For example, with thermal nozzles one must wait for the heater to cool to a desired temperature and for the ink chamber to be refilled before another ejection cycle. Depending on these hardware limitations, the checkerboard design may not be desirable.

Though limited, previous open literature has made significant contributions to designing *PMs*. Yen et al. [1] used unique, asymmetric, complementary 4 by 4 triangular clusters in designing *PMs* to avoid banding. A smooth dithering matrix was used to guide ink migration (i.e. drop coalescence) into patterns that are not perceivable to the human eye. The techniques used in [1] resulted in a group of *PMs* which are admissible under the constraint of the human vision model, but the resulting group may not include all *PMs* which satisfy the constraint.

In a subsequent work [2], *PM* design was formulated as a constrained optimization problem and solved by finding initial solutions with a greedy algorithm with some randomization; then neighborhood searches are used to find local near-optima. The approach is useful in automating the selection of an appropriate print mask. However, since only a single *PM* is selected with some randomness, the insight gained by realizing all admissible *PMs* is still left desired. In addition, the details of mapping a pass number of an image pixel to a nozzle on the print-head as well as course of action used for determining the constraints and cost functions are not mentioned in [2].

Given a printing system, this study formulates a constrained optimization problem to generate all admissible *PMs* that maximizes throughput (i.e. minimizes the number of passes) subject to constraints reflecting hardware limitations and print quality requirements. A drop coalescence constraint incorporating drop placement error and dot gain variations is used as an example of print quality requirements. The details of the constraints used in this paper are given so that the logic can be directly applied to any printing system. In addition, given a print mode and *PM*, a method for mapping the pass number to a nozzle on the print-head for each image pixel is provided.

The remainder of this paper is organized as follows. First, the formal definitions for print mode, print mask, and nozzle mapping will be given. Next, the problem formulation of this paper will be discussed. Then the *PM* constraints, especially those coming from the hardware limitations and print quality issue previously given. The last section will show an example of the techniques developed herein.

## Print Mode, Print Mask, and Nozzle Mapping

For a given printing system, a print mode can be characterized by the amalgamation of a set of parameters, both adjustable and non-adjustable. The adjustable parameters typically associated with the printing mechanism and methods are

- Print-head scan velocity,  $v_{PS}$
- Number of passes,  $n$
- Bidirectional or unidirectional printing
- Media advance speed,  $v_{MA}$
- Print-head return velocity (for unidirectional only),  $v_R$
- Nozzle advancement distance,  $d$
- Total number of nozzles used,  $k$
- Acceptable probability of coalescence,  $P$

The non-adjustable parameters, typically associated with the print-head, ink, and substrates are

- Image resolution,  $r_i$
- Ink properties
- Substrate properties
- Nozzle resolution,  $b$
- Maximum firing/ejection frequency,  $f_{\max}$
- Distance between nozzle columns,  $a$ .

For the analysis to come, we assume that we are using bidirectional printing, that  $v_{PS}$  and  $v_{MA}$  are constant,  $a > b$  and is not an integer multiple of  $b$ ,  $r_i = b$ , that  $d$  be an integer multiple of  $r_i$ , and more specifically

$$d = \frac{k}{n} \cdot r_i = \frac{k}{n} \cdot b. \quad (1)$$

These assumptions will actually invoke constraints on admissible *PMs* as we will show in the *PM* constraints section.

A *PM* is a  $p_1$  by  $p_2$  matrix containing pass numbers. Each element of the *PM* is an integer anywhere from 1 up to  $n$ , the total number of times that the print-head passes over a given pixel in the image. A *PM* associates each pixel of the image with a pass number. The assumption with this definition is that each pixel of the image will receive at most one drop of ink. This is more constrained than the assumptions used in [1]. Even though the algorithm developed herein is based on the one drop per pixel assumption, it can easily be relaxed and applied to multiple drops per pixel.

Let the binary image (*I*) be of pixel dimension  $m_1$  by  $m_2$ . Typically, we have that  $p_1 \ll m_1$  and  $p_2 \ll m_2$ . When this occurs, the *PM* is tiled up to match the dimensions of the image. We call this resulting tiled matrix the canvas. Figure 3 shows an example of applying a *PM* to an image. Figure 3(a) is an image of the word "HI" to be printed, 3(b) is the binary representation of 3(a), 3(c) is an example print mask to be applied to the image, 4(d) is the canvas resulting from tiling up 3(c) to match the dimensions of 3(b), and 3(e) can be thought of as a logical AND of 3(b) and 3(d).

Print mask associates each image pixel with the pass number during which it will be printed. However, for further analysis we need to know which nozzle is responsible for printing each image pixel. For this we introduce nozzle mapping (*NM*).

For a given print mode and *PM* we define the *NM* in the following way. For all  $i = 1, 2, \dots, \max(p_1, k/n)$  and  $j = 1, \dots, p_2$

$$NM(i, j) = k - PM(\text{mod}(i-1, p_1) + 1, j) \cdot \frac{k}{n} + i - \left( \left[ i \cdot \frac{n}{k} \right] \cdot -1 \right) \cdot \frac{k}{n}. \quad (2)$$

Notice that equation (2) does not depend on the size of the image.

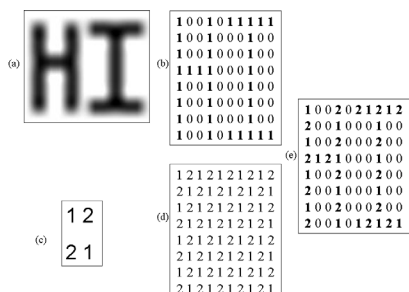


**Figure 3.** PM implementation (a) Input image, (b) Binary image, (c) PM, (d) Canvas, (e) Output image with pass numbers.

To help illustrate how *NM* works, we will apply the algorithm to the example in Figure 3. Figure 4 shows the result of applying the *NM* algorithm to the example in Figure 3 with  $k = 12$ .

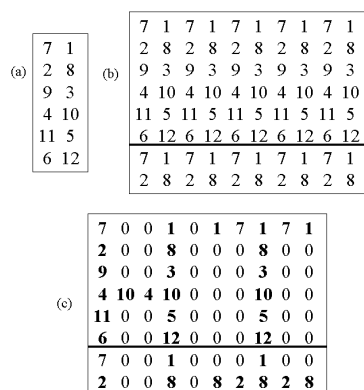


**Figure 4.** NM Implementation (a) NM, (b) Tiled NM, (c) Output Image with Nozzle Assignments.

The horizontal black line is the boundary between print-head advancements in the media advance direction. The size of  $NM$  is  $\max(p_1, k/n)$  by  $p_2$ . This is the maximum size that  $NM$  can reach before it begins to repeat rows or columns. The size of  $NM$  is typically smaller than the size of  $I$ . So, we must tile up  $NM$  in a manner similar to the way we tile up  $PM$  (see Figure 4(b)). Once we have the tiled  $NM$ , we can perform a logical AND with  $I$  (see Figure 4(c)). With  $NM$  now defined, we can move on to implementing the  $PM$  constraints.

## Problem Formulation

Considering all of the adjustable parameters in a print mode, the number of possible print modes and corresponding *PMs* are endless. However, if the print mode and the size of the *PM* are set, then the total number of possible *PMs* is  $n^{p_1 \cdot p_2}$ . The proposed approach iterates through all possible *PMs* of a fixed size for a fixed print mode, eliminating the *PMs* which do not satisfy the constraints. The result is a set of admissible *PMs*. Formally; the problem can be stated as follows.

Given all parameters in the print mode except for  $n$  (i.e. given  $v_{PS}$ , bidirectional or unidirectional printing,  $v_{MA}$ ,  $v_R$  (unidirectional only),  $d$ ,  $k$ ,  $P$ ,  $r_i$ , ink properties, substrate properties,  $b$ ,  $f_{\max}$ , and  $a$ ) and the  $PM$  dimensions  $p_1$  and  $p_2$ , find all  $PM$ s that minimize  $J = n$ , subject to constraints to account for hardware limitations and print quality requirements. The optimization method used is exhaustive enumeration and the details for formulating the constraints are given in the sections to come.

Each admissible  $PM$  is unique but may not be its minimum representation. For example, Figure 2(d) is the minimum representation of Figure 2(a). In other words, Figure 2(a) can be produced simply by tiling up Figure 2(d) and truncating rows and columns so that the matrix dimensions match. For implementation, the minimum  $PM$  representation is of interest. An additional step is needed to find the minimum representation of an admissible  $PM$  prior to implementation.

## Hardware Limitations

There are many hardware limitations which can restrict the number of admissible  $PMs$  for a given print mode. Constraints can be formulated to reflect hardware limitations. This section shows how to formulate constraints to account for hardware limitations stemming from the nozzle advancement,  $d$ , the nozzle geometry, and the maximum firing frequency,  $f_{\max}$ .

### Constraints from nozzle advancement

The assumptions that  $r_i = b$ ,  $d$  be an integer multiple of the image resolution, and equation (1) give way to two constraints on  $n$ . First,  $n$  must be an integer factor of  $k$ ; otherwise, by equation (1) we would not satisfy the assumption that  $d$  is an integer multiple of the image resolution. The second constraint from these assumptions is that  $N = k$ . If  $N > k$ , then by equation (1)  $d$  would no longer be an integer multiple of the image resolution.

To avoid the trivial situation where a pass is associated with no nozzle firing, the following constraint is needed.

$$\bigcup_{i,j} \{PM(i,j)\} = \{1, 2, \dots, n\} \quad (3)$$

for  $i = 1, 2, \dots, p_1$  and  $j = 1, 2, \dots, p_2$ .

### Constraints from nozzle geometry and maximum firing frequency

Once drop formation has occurred in a particular nozzle, the print-head must wait  $1/f_{\max}$  seconds before it can trigger that nozzle again. Therefore, we have constraints if

$$v_{PS} > b \cdot f_{\max} . \quad (4)$$

Figure 5 shows a schematic of a single nozzle passing over a row of pixels in the print-head scan direction at a speed  $v_{PS}$ . Here,  $l$  is the distance traveled between consecutive firing of the same nozzle. Given the maximum firing frequency  $f_{\max}$ ,  $l$  is lower bounded, i.e.

$$l \geq \frac{v_{PS}}{f_{\max}}. \quad (5)$$

Given  $l$ , the number of pixels between two consecutive firings of the same nozzle,  $l_p$  is given by

$$l_p = \frac{l}{b} + 1 \geq \frac{v_{PS}}{b \cdot f_{\max}} + 1. \quad (6)$$

In terms of the  $PM$ , this means that for each row in the  $PM$  the spacing between repeated pass numbers must be at least  $l_p$ . This implies that a necessary condition for the horizontal dimension of the  $PM$ , is  $p_2 \geq l_p$  and for the total number of passes of the print mode is  $n \geq l_p$ . However, the following sufficient condition is needed in order to select distinguish an admissible set of  $PM$ s. Let

$$G_{suf} = [PM \quad PM]. \quad (7)$$

For every row  $i$  of  $G_{suf}$ , if

$$\inf_{j=1,2,p_2-1} \{q-j \mid q > j \text{ and } G_{suf}(i,j) = G_{suf}(i,q)\} \geq l_p. \quad (8)$$

for  $i = 1, \dots, p_1$ , then the  $PM$  is admissible with respect to  $f_{max}$ . It should be noted that equations (7) and (8) only consider the  $PM$  and not the image  $I$ .

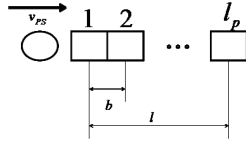


**Figure 5.** Nozzle (circle) traveling over a row of image pixels in the print-head scan direction at a speed  $v_{PS}$

Instead of invoking necessary conditions on the total number of passes,  $n$  and the number of columns of the  $PM$ , we can simply fix  $n$  and  $p_2$ . This would then impose the following necessary conditions on  $v_{PS}$

$$v_{PS} \leq (n-1) \cdot b \cdot f_{max} \text{ and } v_{PS} \leq (p_2-1) \cdot b \cdot f_{max} \quad (9)$$

## Print Quality Requirements

Print quality requirements limit the number of print artifacts (e.g. banding, line raggedness, and drop coalescence) which can occur.  $PM$  constraints can be formulated so that print artifacts are reduced in accordance with print quality requirements. For example, this section formulates  $PM$  constraints for print quality requirements on drop coalescence.

### Coalescence constraints

When two adjacent drops are deposited so that their wetted areas intersect, then coalescence may occur [3]. This affects drop placement error and dot gain. The drop placement error is affected because the centroid of drops will most likely change after coalescence. The dot gain will be increased since during coalescence, two or more drops merge to become one.

In order to avoid coalescence, one must wait a minimum amount of time to allow for a deposited drop to dry and/or absorb into the substrate before depositing an adjacent drop. Any appropriate model for drops impacting on a substrate, drying on a substrate, and absorbing into a substrate can be used. A previously developed model [3] considered the effects of drops spreading, receding, and drying on nonporous media while considering nozzle-dependant drop placement errors. Because the drop placement error is a function of the nozzle in the print-head, we have chosen to make the timing constraint also a function of the nozzles.

In many printing applications, print quality can be characterized by an acceptable probability,  $P$  of coalescence between adjacent drops. For critical print jobs such as printed

circuits we wish for  $P = 0$  so that we do not risk any open or shorted circuits. However, for applications such as halftoned images we can accept a higher probability of coalescence. Therefore, we have chosen to make the timing constraint between adjacent drops be a function of the probability of coalescence.

To find the time of drop deposition for an image pixel it is advantageous to know at what advancement of the print-head in the media advance direction that the deposition occurs. The time it takes to arrive at print-head advancement  $i$  for any  $i = 1, 2, \dots, A = (2 \cdot k - k/n) \cdot n/k + n - 1$  can be computed by

$$T_i = (i-1) \cdot \left( \frac{2 \cdot \varepsilon + a}{v_{PS}} + \frac{b \cdot \frac{k}{n}}{v_{MA}} \right); \quad (10)$$

where

$$\varepsilon = \delta + v_d \cdot h; \quad (11)$$

where  $v_d$  is the velocity of the drop during flight perpendicular to the substrate, assumed to be constant and  $h$  is the distance between the substrate and the print-head, assumed to be constant.  $\delta$  is the distance that the print-head travels before reaching the extents of the image  $\pm v_d \cdot h$  (+ if the print direction is from right to left and - if the print direction is from left to right). It should be noted that equation (10) assumes that the image width  $m_2$  is only 1 and the image height  $m_1$  is  $2 \cdot k - k/n$ . By assumption, equation (10) is a conservative approach.

Once the print-head advancement is known for an image pixel, we can then compute the pixel's time of deposition. Let  $ad$  be the print-head advancement ( $i, j$ ) be the pixel location, and  $c$  be the nozzle array column responsible for depositing ink. Then the deposition time for an image pixel is

$$T_{ij} = T_{ad} + \varsigma_1 + \varsigma_2. \quad (12)$$

The first term on the right hand side of equation (12) represents the time it takes for the print-head to travel to the print-head advancement of the image pixel. The second term on the right hand side of equation (12) is the time associated with reaching the  $j$ th column of the image and can be computed by

$$\varsigma_1 = \begin{cases} \frac{\varepsilon + b \cdot (j-1)}{v_{PS}} & \text{if the print direction is from left to right} \\ \frac{\varepsilon + b \cdot (2 \cdot p_2 - j)}{v_{PS}} & \text{if the print direction is from right to left} \end{cases}. \quad (13)$$

Equation (13) is conservative because it assumes that the image width  $m_2$  is the same as twice the  $PM$  width,  $p_2$ . The last term on the right hand side of equation (12) represents the time associated with the staggered nozzle geometry of the print-head and can be computed by Table 1.

**Table 1: Computation details for  $\varsigma_2$**

c	Print Direction	
	Left to Right	Right to Left
1	$a/v_{PS}$	0
2	0	$a/v_{PS}$

For each image pixel  $I(i, j)$ ,  $i = 2, 3, \dots, 2 \cdot k - k/n$ ,  $j = 1, 3, \dots, 2 \cdot p_2$ , and for each  $w = 1, 2, 3, 4$  we compute the deposition time difference  $|T_{ij} - T_w|$  between pixel  $(i, j)$  and its four neighbors as shown in Figure 6. The remaining four neighbors in Figure 6 are

not considered because they will by definition be considered in later values of  $i$  and  $j$ .  $|T_{ij} - T_w|$  can be computed using equations (10) – (13) and Table 1. Since  $|T_{ij} - T_w|$  depends on the nozzles responsible for deposition, we must tile up  $NM$  to be of size  $2 \cdot k \cdot k / n$  by  $2 \cdot p_2$ . In addition to computing  $|T_{ij} - T_w|$ , we must compute the threshold deposition time difference,  $T_{\min}$ . The coalescence model described in [3] has been chosen to calculate  $T_{\min}$ , which depends on the nozzles responsible for deposition, the desired center-to-center distance between drops, and the acceptable probability of coalescence. Therefore,  $T_{\min} = T_{\min}(w, i, j, P)$ . After computing  $|T_{ij} - T_w|$  and  $T_{\min}(w, i, j, P)$ , the following coalescence constraint can be applied.

$$|T_{ij} - T_w| \geq T_{\min}(w, i, j, P). \quad (14)$$

If equation (14) is satisfied for all  $i, j$ , and  $w$ , then the  $PM$  is admissible with respect to the coalescence constraint.

$T_1$	$T_2$	$T_3$
$T_4$	$T_{ij}$	

**Figure 6.** Schematic of image pixel  $(i, j)$  and its adjacent pixels with their corresponding deposition times.

As an example, we apply the time constraint for coalescence to the example image and  $PM$  shown in Figure 3 and Figure 4. To illustrate the implementation of the coalescence constraint example computations are provided in Figure 7, where  $i = j = 2$ ,  $P = 0.8$ ,  $a = 273 \mu\text{m}$ ,  $b = 70.55 \mu\text{m}$ ,  $v_{PS} = v_{MA} = 10^3 \mu\text{m/s}$ , and it is assumed that  $2\epsilon \ll a$ . Figure 7(a) shows the nozzles responsible for printing the first neighbor through the fourth neighbor and pixel  $(i, j)$ . Figure 7(b) shows  $|T_{22} - T_w|$ . Figure 9(c) shows  $T_{\min}(w, 2, 2, 0.5)$ . The values for Figure 7(c) can be obtained from the plot shown in Figure 8, which was generated by appropriately applying the coalescence model in [3]. The parameter values used in the coalescence model for the simulations in this study are the same as those used in [3]. For this particular pixel ( $i=j=2$ ), the  $PM$  is admissible. However, this process must be repeated for all values of  $i$  and  $j$  before it can be determined if the  $PM$  is admissible with respect to the coalescence constraint.

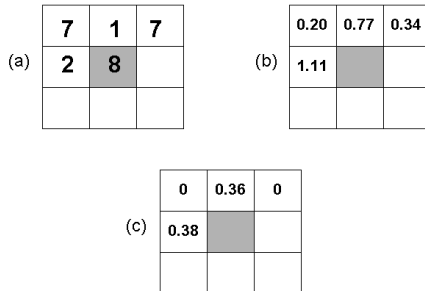


**Figure 7.** Example of coalescence constraint implementation for  $i = j = 2$ : (a) Nozzle assignments, (b)  $|T_{22} - T_w|$ , and (c)  $T_{\min}(w, 2, 2, 0.8)$ .

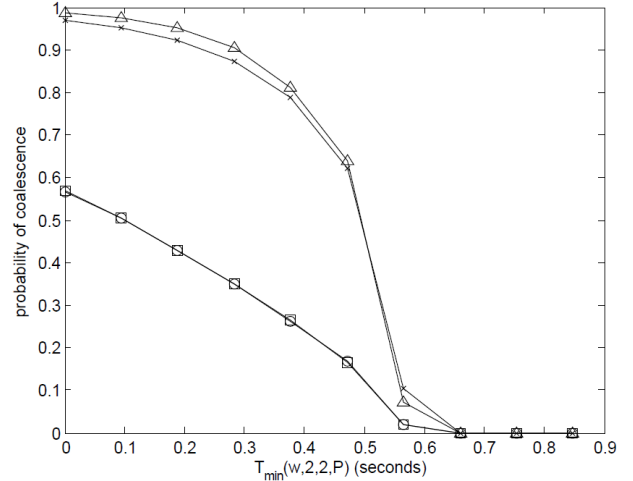


**Figure 8.** Example plot of probability of coalescence versus time: (○) Upper left neighbor, (×) Upper middle neighbor, (□) Upper right neighbor, and (Δ) Middle left neighbor [3].

As currently described, the coalescence constraint is a sufficient condition. To make the coalescence constraint both necessary and sufficient, one must consider the image,  $I$ , to be printed.

## Examples

With the constraints defined, the problem formulation is as follows.

Given:

- Print mode parameters except for the number of passes  $n$
- Print mask dimension:  $p_1$  and  $p_2$

Find: All admissible  $PM$ s which minimize  $n$

Subject to:

- $n$  is an integer factor of  $k$
- $n \leq k$
- equations (3), (8), and (14)

In this section, two examples of ejecting water on glass substrate will be used to illustrate the utility of these methods. Both examples assume a  $3 \times 2$  print mask, i.e.  $p_1 = 3$ ,  $p_2 = 2$ , and the following print mode parameters.

- $v_{PS} = 10^3 \mu\text{m/s}$
- bidirectional printing
- $v_{MA} = 10^3 \mu\text{m/s}$
- $r_i = 70.55 \mu\text{m}$
- ink properties equivalent to that in [3]
- substrate properties equivalent to that in [3]
- $b = 70.55 \mu\text{m}$
- $f_{\max} = 45 \text{kHz}$
- $a = 273 \mu\text{m}$

An iterative search will be conducted for both examples. The first example considers print quality requirements which allow for  $P = 0.91$ , i.e. 91% acceptable coalescence. The second example considers print quality requirements which allow for  $P = 0.59$ , i.e. 59% coalescence.

The iterative search for  $P = 0.91$  results in 4 admissible print masks,

$$PM_{0.91}1 = \begin{bmatrix} 1 & 2 \\ 2 & 1 \\ 1 & 2 \end{bmatrix}, \quad PM_{0.91}2 = \begin{bmatrix} 1 & 2 \\ 2 & 1 \\ 2 & 1 \end{bmatrix}, \quad PM_{0.91}3 = \begin{bmatrix} 2 & 1 \\ 1 & 2 \\ 1 & 2 \end{bmatrix}, \quad \text{and}$$

$$PM_{0.91}4 = \begin{bmatrix} 2 & 1 \\ 1 & 2 \\ 2 & 1 \end{bmatrix}.$$

As one can see, the minimum number of passes for this quality requirement is  $n = 2$ , i.e. a two pass print mode.

The iterative search for  $P = 0.59$  resulted in 2 admissible print masks,

$$PM_{0.59}1 = \begin{bmatrix} 2 & 4 \\ 4 & 1 \\ 1 & 3 \end{bmatrix} \quad \text{and} \quad PM_{0.59}2 = \begin{bmatrix} 4 & 2 \\ 1 & 4 \\ 3 & 1 \end{bmatrix}.$$

The minimum number of passes to satisfy this quality requirement is  $n = 4$ .

Note that for large images, i.e.  $m_1 \gg 3$  and  $m_2 \gg 2$ ,  $PM_{0.91}1$  is effectively the same as  $PM_{0.91}3$ ,  $PM_{0.91}2$  is effectively the same as  $PM_{0.91}4$ , and  $PM_{0.59}1$  is effectively the same as  $PM_{0.59}2$ . These  $PMs$  are one row or column permutation from one another. The fact that the proposed methods cannot distinguish these  $PMs$ , indicated that additional constraints will need to be included so that effective  $PMs$  are not repeated in the admissible set.

## Conclusions

Given a printing system, this study has formulated a constrained optimization problem to generate all admissible print masks that maximize throughput (i.e. minimizes the number of passes) subject to constraints reflecting hardware limitations and print quality requirements. Details for formulating constraints from hardware limitations such as the nozzle advancement, nozzle geometry and maximum firing frequency as well as constraints from the print quality requirement of drop coalescence have been given. Two examples have been provided to show the utility of these methods. Consideration/constraints to incorporate additional print quality requirements and combine redundant  $PMs$  in the admissible set are being investigated.

## References

- [1] J. Yen, Q. Lin, and P. Wong, "Print Masks for Inkjet Printers," US Patent 5,992,962 (1999).
- [2] J. Yen et al., "Constraint Solving for Inkjet Print Mask Design," *Jour. Imaging. Sci. and Technol.*, 44, 391 (2000).
- [3] J. Boley, K. Ariyur, and G. Chiu, "Coalescence Constraints for Inkjet Print Mask Optimization," *AIM*, (2010).

## Author Biography

*J. William Boley received a BS with a double major in Mechanical Engineering and Mathematics as well as an MS in Mechanical Engineering from the University of Kentucky. He is currently pursuing a Ph.D. in the School of Mechanical Engineering at Purdue University.*